Superconductivity and Cryogenics
Vol.15, No.2, (2013), pp.1~8 http://dx.doi.org/10.9714/psac.2013.15.2.001

Magnetic refrigerator for hydrogen liquefaction

T. Numazawa[a], K. Kamiya[b], T. Utaki[c, d], and K. Matsumoto[e]

[a] *National Institute for Materials Science, Tsukuba, Japan*
[b] *Japan Atomic Energy Agency, Naka, Japan*
[c] *Osaka University, Osaka, Japan*
[d] *Currently, Osaka Gas Co., Ltd., Osaka, Japan*
[e] *Kanazawa University, Kanazawa, Japan*

(Received 28 June 2013; revised or reviewed 29 June 2013; accepted 30 June 2013)

Abstract

This paper reviews the development status of magnetic refrigeration system for hydrogen liquefaction. There is no doubt that hydrogen is one of most important energy sources in the near future. In particular, liquid hydrogen can be utilized for infrastructure construction consisting of storage and transportation. Liquid hydrogen is in cryogenic temperatures and therefore high efficient liquefaction method must be studied. Magnetic refrigeration which uses the magneto-caloric effect has potential to realize not only the higher liquefaction efficiency > 50 %, but also to be environmentally friendly and cost effective. Our hydrogen magnetic refrigeration system consists of Carnot cycle for liquefaction stage and AMR (active magnetic regenerator) cycle for precooling stages. For the Carnot cycle, we develop the high efficient system > 80 % liquefaction efficiency by using the heat pipe. For the AMR cycle, we studied two kinds of displacer systems, which transferred the working fluid. We confirmed the AMR effect with the cooling temperature span of 12 K for 1.8 T of the magnetic field and 6 second of the cycle. By using the simulation, we estimate the total efficiency of the hydrogen liquefaction plant for 10 kg/day. A FOM of 0.47 is obtained in the magnetic refrigeration system operation temperature between 20 K and 77 K including LN_2 work input.

Keywords : Magnetic refrigeration, Magnetocaloric effect, Hydrogen, Liquefaction

1. INTRODUCTION

Hydrogen has been considered as one of the most clean energy resources and also useful cold refrigerant for superconducting technologies operating > 20 K. Using the hydrogen in our society, one of key issues is the infrastructure construction consisting of hydrogen generation, liquefaction, storage and transportation.

Liquid hydrogen has a higher density than that of gaseous one, so it is great advantage for storage and transportation. However, the liquid hydrogen has a cryogenic temperature ~20 K, so we must consider the high efficient liquefaction method and the adiabatic storage with safety.

There are many hydrogen liquefaction plants and they have achieved quite high FOM (=figure of merit) as much as ~0.4, but this value is not enough to use for the hydrogen applications at room temperatures. When we compare the consuming energy of hydrogen liquefaction with high pressurized hydrogen gas (typically 70 MPa), we notice that FOM must be larger than 0.5 for hydrogen liquefaction at least [1]. This is the reason why we need to develop more efficient refrigeration system for hydrogen liquefaction.

Magnetic refrigeration method makes use of the magnetocaloric effect (MCE) where some magnetic materials exhaust or absorb heat by applying or removing external magnetic fields. MCE is induced by the internal magnetic entropy change of magnetic materials and it occurs through the magnetic material with a lighting speed, thus magnetic refrigeration can operate an ideal cycle like Carnot. Another advantage of magnetic refrigeration is to use the solid magnetic materials, which have typically 1000 times higher entropy density than that of gas. Magnetic refrigeration system is environmentally friendly, quiet operation and possible more efficient than conventional liquefaction methods.

In this review paper, we will describe the experimental system for Carnot and AMR cycles with magnetic materials and magnet. Also some simulation results for the whole refrigeration system will be shown to predict the future development of hydrogen magnetic refrigeration.

2. SCHEME OF HYDROGEN MAGNETIC REFRIGERATION CYCLE

To realize a hydrogen liquefaction cycle by using a magnetic refrigerator, we need several cascaded cycles to cover wide temperature ranges from heat source temperatures to liquid hydrogen temperature (20.3 K). The source temperature is usually set at room temperature, but we also can consider the use of liquid natural gas = LNG (112 K) or liquid hydrogen (77 K) for connecting to the magnetic refrigerator. This is because a number of LNG plants have been built in Japan for the energy source and LNG also can be used as a hydrogen source. Since the

* Corresponding author: uumazawa.takenori@gmail.com

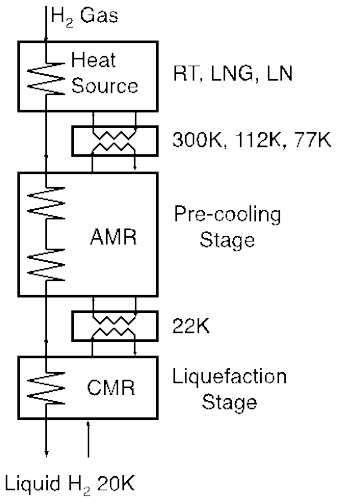

Fig. 1. Hydrogen gas flow circuit of hydrogen liquefaction cycle for the magnetic refrigeration, consisting of CMR and AMR.

temperature of LNG is already cold, LNG will contribute largely to improve the efficiency of the hydrogen magnetic refrigerator cycle [2].

Fig. 1 shows a typical gas flow circuit of the hydrogen liquefaction cycle of the magnetic refrigeration. There are two kinds of magnetic refrigeration cycles; CMR = Carnot Magnetic Refrigerator and AMR = Active Magnetic Refrigerator. Hydrogen gas is precooled to the temperature slightly above the boiling point with an AMR, and then it is liquefied with a CMR. Since the CMR provides a temperature span of a few degrees, another AMR must be connected to the CMR to absorb the exhausted heat. AMR can provide large refrigeration temperature span, but usually we need to cascade several units of AMR to reach ~ 22 K.

3. CARNOT CYCLE FOR LIQUEFACTION STAGE

3.1. Liquefaction Principal

For the liquefaction stage by the CMR, we use a heat pipe to condense the hydrogen gas by the magnetic material. This method achieves considerably higher thermal efficiency compared with the conventional method using the Joule-Thomson valve. Fig. 2 shows the details that hydrogen gas is condensed directly on the surface of the magnetic materials, subsequently liquid hydrogen drops downwards to reservoir. The principal is equivalent to a thermo-siphon, a type of a heat pipe, and categorized into the heat transport regime making use of the gravity unlike the normal thermo-siphon uses capillary phenomena for liquid circulation. This method makes use of the phase transition from gas to liquid and therefore, it's heat transfer rate is comparable to that of copper material.

3.2. Experimental System

Fig. 3 shows CMR test apparatus consisting of magnetic refrigerant, a 6 T superconducting magnet and a heat

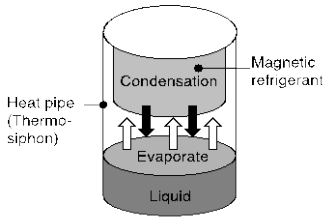

Fig. 2. Liquefaction principal of magnetic refrigerator based on thermo-siphon method.

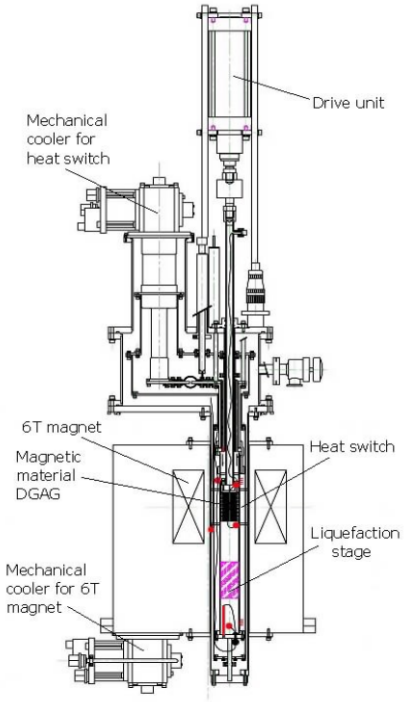

Fig. 3. CMR test apparatus consisting of magnetic material, superconducting magnet, heat switches and drive unit.

switch [3]. The magnetic field applied on the magnetic refrigerant is varied by moving the refrigerant (0.28 kg of dysprosium gadolinium aluminum garnet, DGAG) by 15 cm in the magnet with a drive shaft connected to a displacer. Since the superconducting magnet is a solenoid type of a magnet without a bucking coil, the magnetic field only reduces to 1 T at 15 cm away from the magnet center. However, DGAG exhibits large entropy change at higher magnetic field, 15cm stroke shouldn't matter.

In Fig. 3, at the start of the cooling cycle, DGAG, initially at the center of the magnet, starts to move downwards to a shaded area called a liquefaction stage decreasing its temperature by the magnetocaloric effect. Hydrogen gas filling the liquefaction stage starts liquefying when DGAG temperature dips from the liquefaction temperature. After a certain period, DGAG starts to move back to the original magnet center increasing its temperature. Heat from DGAG is transferred at the magnet center with a gas-gap heat switch connected to a conventional G-M mechanical cryocooler. For our

refrigerator, the operation frequency is adjustable from 0.01 Hz to 0.5 Hz.

As for a thermal aspect of the refrigerator, drive shaft is one of the critical components because the top of the shaft is exposed to the room temperature and the bottom is at liquid hydrogen temperature, 20 K. In addition, the shaft brings shuttle heat transfer by moving up and down. In order to minimize the heat leak, the two different materials – stainless for upper half the shaft and FRP for lower the shaft – are used for the drive shaft because the upper shaft is closed up with the Wilson seal.

3.3. Magnetic Materials

In general, rare-earth metallic compounds such as $ErAl_2$ provide large entropy changes in the temperature range of 20 K-77 K, but these materials absorb easily the hydrogen. Usually this kind of phenomena results to decompose the materials and change them to powders. For the liquefaction process, the best way is to condense the hydrogen gas directly on the surface of the magnetic material, so we need to develop the materials without any decomposition. In this study, we have newly developed a ceramic magnetic refrigerant, dysprosium gadolinium aluminum garnet, DGAG to avoid this difficulty [3]. A reason why Gd is added is that garnets including Gd tend to be magnetically isotropic since Gd ion is generally localized in the garnet crystal structure due to no LS coupling. In addition, adding the Gd increases the zero magnetic field entropy because of the large magnetic moment of the Gd ion; J=7/2. These are important factors to enhance the magnetocaloric effect. Fig. 4 shows the entropy diagram for the poly crystal 20%DGAG.

In order to maximize the surface area of DGAG and in order for hydrogen gas to flow without large pressure loss, DGAG is formed in slit shape as seen in Fig. 5. Thus, the whole DGAG holder consists of a copper hollow cylinder and rectangular solid DGAGs line up in parallel to each other with a gap of 1mm. The holder is also placed in parallel to hydrogen flow direction.

3.4. Experimental Results

In our experiments, hydrogen liquefaction is judged from the temperature variation with thermometers on

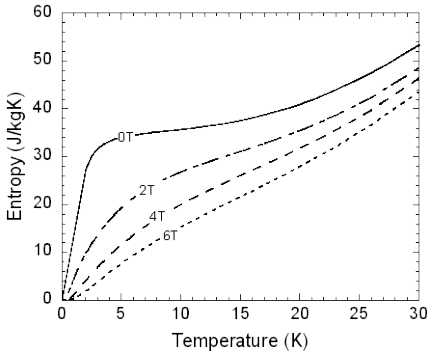

Fig. 4. Entropy diagram of poly crystal 20%DGAG at several magnetic fields.

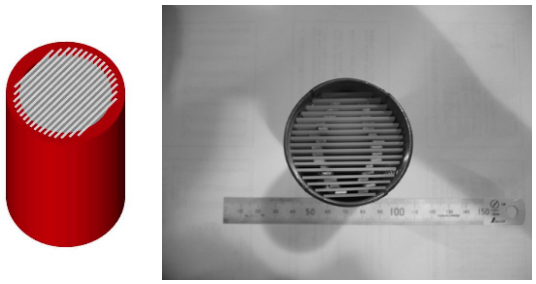

Fig. 5. A cross shot of its schematic drawing (left) and a picture of DGAG holder from the top view (right).

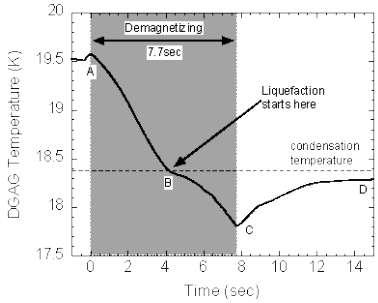

Fig. 6. The temperature variation of the DGAG in the liquefaction process. The magnetic field is varied for 7.7 seconds in a gray area. A discontinuity point indicates liquefaction starts.

DGAG due to lack of an appropriate commercial level detector matches our small experimental cell [3-4]. Fig. 6 shows DGAG temperature variation during liquefaction process. Grey area indicates demagnetizing process and a broken line is the hydrogen condensation temperature (boiling point) under corresponding saturated vapor pressure. It is seen in Fig. 6 that the DGAG temperature starts decreasing onset of demagnetization at the point A due to magnetocaloric effect, and ends decreasing at the end of demagnetization pointed by C. In the demagnetization process, discontinuity in the temperature slope indicated by B is seen in Fig. 6. Since the DGAG temperature at this discontinuity coincides with the hydrogen condensation temperature indicated by the broken line in the Fig. 6, we conclude that this discontinuity point means beginning of liquefaction.

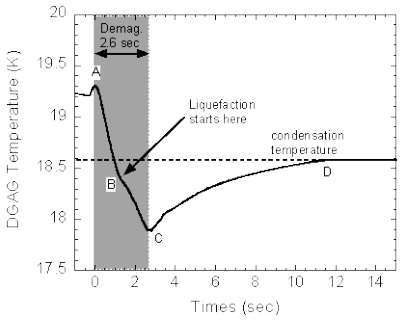

Fig. 7. The temperature variation of DGAG in the liquefaction process at the speed of 2.6 sec demagnetization. It is seen that hydrogen is supercooled due to too fast demagnetization.

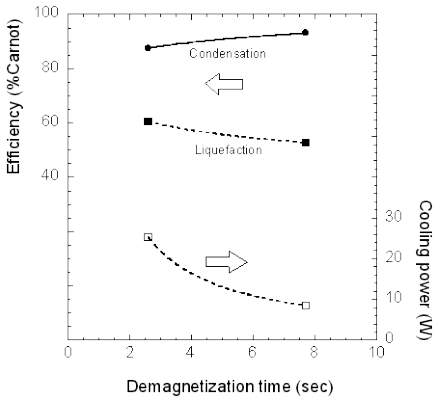

Fig. 8. The efficiency in condensation and liquefaction process estimated from the entropy diagram. The cooling power in liquefaction process also calculated.

Fig. 7 shows the DGAG temperature variation at a different demagnetization speed. In Fig. 7, a discontinuity point B is seen to come to below the condensation temperature. This is because hydrogen undergoes supercooling state due to too fast demagnetization. In addition, it is also seen in Fig. 7 that the DGAG temperature quickly comes up to its condensation temperature.

The efficiency and the cooling power of our magnetic refrigerator in the liquefaction process are estimated as shown in Fig. 8. It was found that the condensation efficiency reaches 90% Carnot and even the liquefaction efficiency accomplishes higher than 50% Carnot. The liquefaction power is found to decrease with demagnetization time and the maximum power was 25.3W.

4. AMR CYCLE FOR PRECOOLING STAGE

4.1. AMR Cycle

AMR cycle is widely used in the higher temperature range where the adiabatic demagnetization temperature changes to be smaller due to increasing the lattice entropy. The operation of AMR cycle is very simple as shown in Fig. 9. The AMR cycle consists of four portions including magnetic field changes and internal heat flow by the heat exchange fluid. This cycle is based on the regenerator used in cryocoolers, but most different point is that the magnetic regenerator material behaves to absorb or exhaust the heat actively by the MCE, so the phenomena occurred in the AMR is more complex than that of the static regenerator. For the operation of AMR cycle, we have two ways to move the heat exchange fluid by the displacer; build-in and external ones. Fig. 10 shows the schematic of both systems. The displacer is one of most difficult parts in the AMR as shown later.

4.2. Experimental System

Our experimental system of AMR is quite similar to the CMR test apparatus, but it has a displacer. First we studied the build-in displacer system because of the simplicity, and then upgraded the system to the external one.

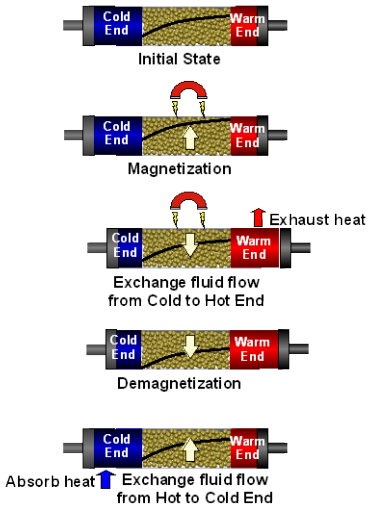

Fig. 9. Operation of AMR cycle consisting of magnetic field change and heat flow process.

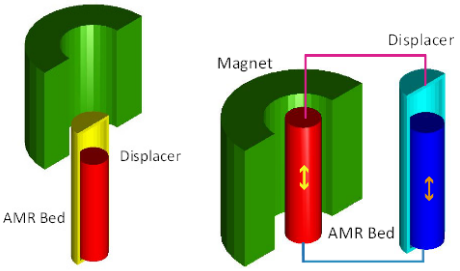

Fig. 10. Schematic of build-in displacer AMR (left) and external displacer AMR (right).

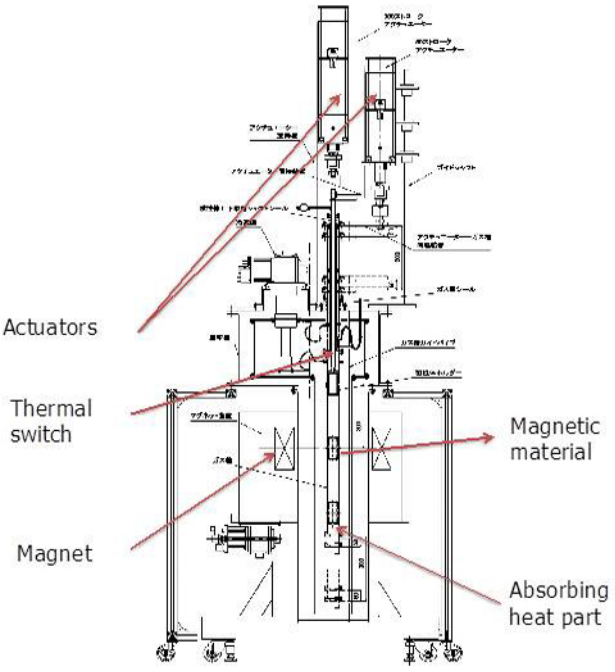

Fig. 11. Test apparatus for the build-in type AMR.

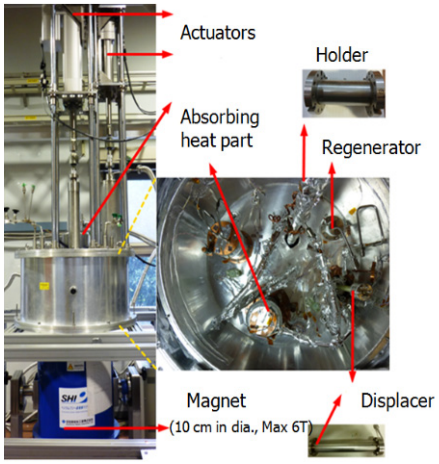

Fig. 12. Test apparatus for external displacer AMR.

Fig. 11 shows the test apparatus for the build-in type. Two actuators were used to move the magnetic material and heat transfer gas. The typical stroke of actuator was 200 mm and maximum speed of the cycle was 6 seconds. We used a large conduction cooled magnet whose bore size and maximum magnetic field were 30 cm at room temperature and 4 T respectively. But this magnet had a considerably large magnetic field leakage, so even for 20 cm away from the center of the magnet, about 40 % of magnetic field remained. Thus, we had to operate the net magnetic field as 1.8 T with the maximum magnetic field of 3 T. As the heat transfer gas, we used the helium with the maximum pressure of 0.25 Mpa.

The merit of this type is that we can put the displacer closer to the magnetic material, so the void volume of the heat transfer fluid is very small. But it is difficult to make effective heat exchangers for both absorbing and exhausting the heat. Also, the bore size becomes larger. On the other hand, as shown in Fig. 12, the external system can put the heat exchanger easily away from the magnetic material, but the void volume of in the pipes connecting between the magnetic material and the heat exchangers becomes larger, and also it is difficult to realize the displacer which has to transfer enough volume of heat transfer fluids in low temperatures.

In order to avoid this kind of difficulty, two approaches have been studied elsewhere [7-8]. Both studies used the gas compressor to transfer the heat exchange gas at room temperature and the gas is precooled by liquid nitrogen or cryocooler. This method has advantage to transfer enough amount of gas with high pressure, but the temperature stability becomes small. Precooling of heat transfer gas is one of most key issues in hydrogen magnetic refrigeration and we need more experience to fix this problem.

4.3. Magnetic Materials

Rare earth intermetallic compounds are good refrigerants because their large angular momentum J tend to produce large entropy changes by magnetic field. RM_2 (R: rare earth, M: Al, Ni, Co) is a Laves phase compound. Transition temperature can be controlled by the change of R and/or M. In Fig. 13, we show magnetic phase transition

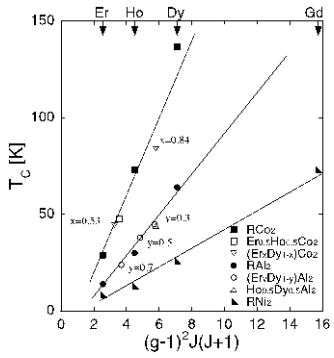

Fig. 13. Magnetic phase transition temperatures for various RM2 (M: Ni, Al, Co) compounds as functions of de Gennes value.

temperatures as functions of de Gennes value for the series of RNi_2, RAl_2, and RCo_2. The substitution of one magnetic lanthanide for the original lanthanide raises or lowers the phase transition temperature as one expect from the respective de Gennes values in Fig. 13 [5]. We measured magnetic and thermal properties. RNi_2, RAl_2 compounds have a second order phase transition from paramagnetic to ferromagnetic state. The entropy change has a peak around Tc in every field, doesn't saturate up to 5 T and gradually lowered both below and above Tc. RCo_2 (R: Dy, Ho, and Er) exhibit a first order paramagnetic-ferrimagnetic phase transition. Above the transition temperature, a field-induced metamagnetic transition occurs. We have studied the effect of substituting one magnetic lanthanide for the original lanthanide, such as $(Er_xHo_{1-x})Co_2$ and $(Er_xDy_{1-x})Co_2$ because these substitution would keep the transition as first order. Entropy change ΔS was saturated with moderate field. The temperature region of large ΔS was broadened to high temperature with increasing field due to the metamagnetic transition. These behaviors of ΔS are characteristic of the first order magnetic transition. The problem on those materials is to absorb the hydrogen largely and occur the decomposition by the hydrogenaration. We have several solutions to avoid this. Typical way is to use the coating on the surface of the materials.

As shown in section 3.3, garnet magnetic materials do not have such a kind of issue, but the entropy change of these materials becomes smaller in the temperatures > 20 K. We developed the rare earth garnet, Fe-modified gadolinium gallium garnets ($Gd_5(Ga_{1-x}Fe_x)_5O_{12}$=GGIG) to provide the larger entropy change by adding the Fe element to enhance the magnetic interaction [6]. We confirmed that the GGIG provided the larger entropy change than that of the DGAG, but the value becomes smaller for > 25 K. We may use the GGIG to extend the temperature region with the DGAG < 25 K.

4.4. Experimental Results

First, we will show the experimental results for the build-in displacer AMR system. Three materials, GGIG (Fe=50%), $HoAl_2$ and $DyAl_2$ were tested. Fig. 14 and Fig.

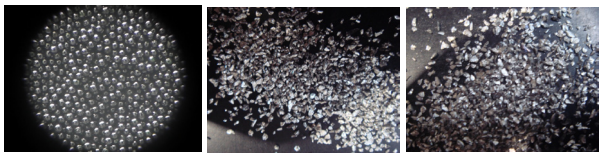

Fig. 14. Photographs of left: GGIG (Fe=50%), center: $HoAl_2$ and right: $DyAl_2$.

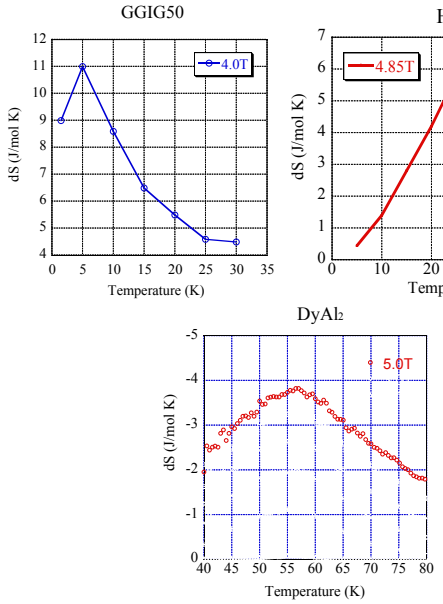

Fig. 15. Entropy changes of top-left: GGIG (Fe=50%), top-center: $HoAl_2$ and bottom: $DyAl_2$.

15 shows the photographs and entropy changes of these materials. At that moment, we could fabricate the sphere materials only for garnet ones, so we used the crashed chips screened with 0.4 mm mesh filter for the $HoAl_2$ and the $DyAl_2$. The reason why we chose these materials was the peak temperature of magnetic entropy change. So, if we operate the AMR cycle from 20 K to 77 K, we have to use three layers with those materials to cover the wide temperature range. Fig.16 shows the AMR cycle operation showing the actual time parameter and Fig. 17 shows the temperature change during the cycle operation. There are two temperatures for hot and cold end of the AMR bed. Left figures show the temperature change in adiabatic condition, i.e., no flow the gas inside. These data should be the same, but we notice the small amount of difference. This comes from the non-uniformity of the AMR bed temperature at the initial condition due to the precooling by conduction. This depends on the apparatus, so we may say this value is a kind of background noise. Right figures show the AMR operation with heat transfer fluid, i.e., helium. The results clearly show the effect of AMR cycle. The difference between hot end and cold end temperatures becomes larger for all materials. Fig. 18 shows the summary of the results on temperature span achieved by the AMR cycle. $HoAl_2$ shows the largest temperature span, but we may not be able to use this material for higher temperatures. Please note that these results were only for 1.8 T of net magnetic field, so it will be expected that 2 or 3 times larger span can be achieved when we use the optimized magnet with 5 T.

For the external displacer system, we built the first model with another superconducting magnet of maximum magnetic field 5 T. This magnet has only 10 cm bore size at room temperature, but the external system does not require a moving part (channel) for heat exchange gas, so it contributes to make the system smaller and heat exchangers for cold and hot parts can be made easily. Fig. 19 shows the photograph of the external system. Since we use the same cryostat as that for build-in model, large void space can be seen in Fig. 12. For the initial test, we faced a severe problem on the cold displacer. We used a polymer sealing (Enerseal) for the displacer, but it did not work well

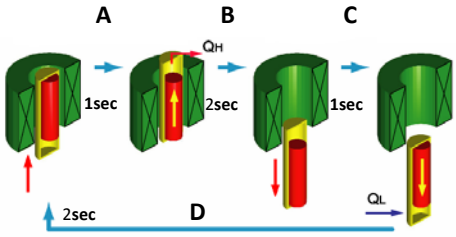

Fig. 16. AMR cycle operation for build-in type. Total cycle period is 6 seconds.

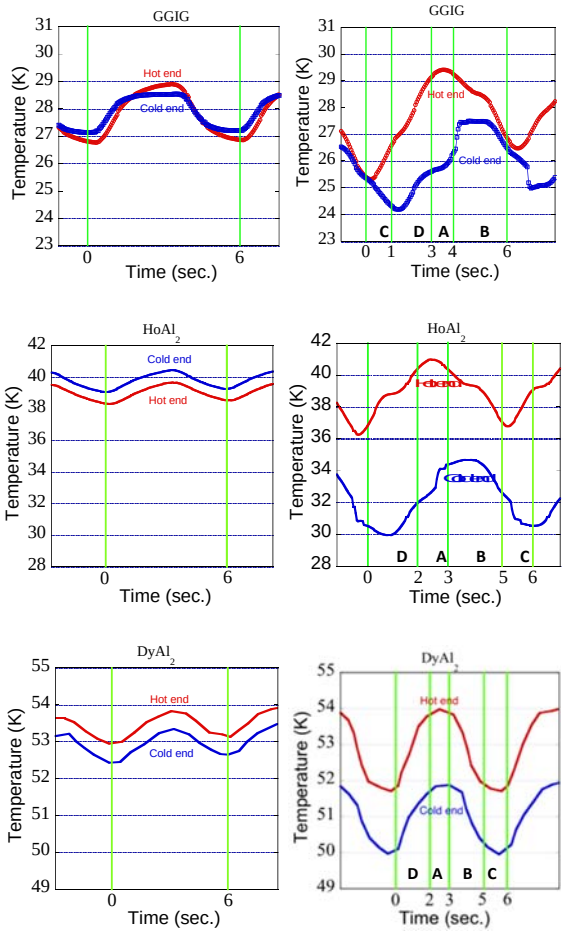

Fig. 17. Temperature change of AMR hot end and cold end during the cycle operation. Top: GGIG (Fe=50%), center: $HoAl_2$ and bottom: $DyAl_2$.

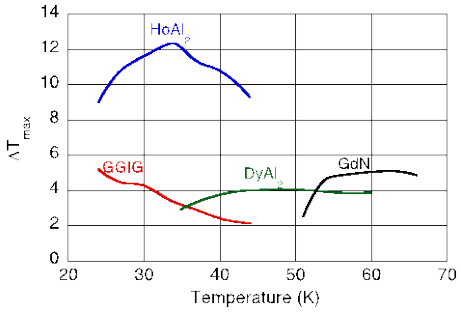

Fig. 18. Summary of the results on temperature span ΔT achieved by the AMR cycle.

at 20 K. Actually we could transfer the enough volume of the gas with low pressures, but the channel between the heat exchangers and AMR bed are narrow, so much higher > 0.1 Mpa must be generated. So far, we could not fix this issue, so our experimental results didn't show any AMR effect. But we confirmed the merit of external displacer system suitable for practical use.

5. SIMULATION FOR HYDRIGEN LIQUEFACTION PLANT

In order to estimate the usability of hydrogen magnetic refrigeration, cycle simulation is one of the important tools. We will show the simulation results on hydrogen liquefaction plants by the magnetic refrigeration.

5.1. Simulation Model

As shown in section 2, our simulation will use the source temperatures at room (atmosphere), liquid nitrogen (LN_2) and liquid natural gas (LNG). By the basic calculation on entropy generation, we assume the number of cooling stages consisting of 4-9 including precooling (AMR) and liquefaction (CMR) ones. This number depends on the source temperature as shown in Fig. 19 and Fig. 20.

The parameters used to perform this work are shown in Table I. Hydrogen gas is supplied at 300 K and pre-cooled to CMR hot end temperature (22 K) by the multi-stages AMR. As hydrogen is precooled by cryogenic liquid as LN_2 or LNG, AMR pre-cools hydrogen from 77 K or 120 K to 22 K. Liquid hydrogen production rate is 10 kg/day. We can calculate that the minimum theoretical work for this production rate is 1.65 kW. Maximum applied field is 5 T. One cycle period is 0.2 sec. Sphere size for packing is 0.2 mm. Working fluid varies by AMR operating temperature range. In this work, we applied hydrogen, liquid propane and ethylene glycol/water as the working fluid as shown in Fig. 19. In our current model, an ideal magnetic material with constant magnetocaloric effect is employed as magnetic working substance. Magnetic entropy change of an ideal magnetic material is a minimum value, 86.2 mJ/cm^3 K, assumed to achieve at all temperature. The conversion of ortho-hydrogen to para-hydrogen is assumed to take place instantaneously, assuming perfect catalysis in the regenerator bed.

Details of simulation already described in elsewhere [2], so we will show only the results here.

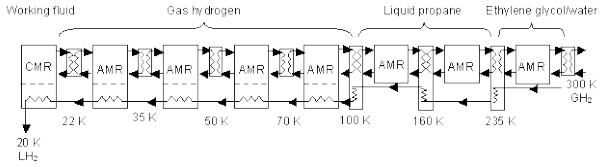

Fig. 19. Magnetic refrigerator for hydrogen liquefaction combined 8 stages AMR with CMR.

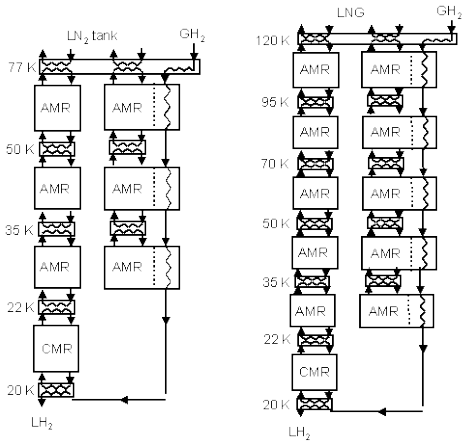

Fig. 20. Left: Magnetic refrigerator for hydrogen liquefaction combined 3 stages AMR with CMR and precooled by LN_2. Right: Magnetic refrigerator for hydrogen liquefaction combined 5 stages AMR with CMR and precooled by LNG.

TABLE I
PARAMETERS USED IN THIS SIMULATION.

Heat rejection temperature	300 K
Load temperature	22 K
Production rate	10 kg/day
Maximum applied field	5 T
Number of AMR beds	6
Cycle period	0.2 sec (5 Hz)
Sphere size for packing	0.2 mm

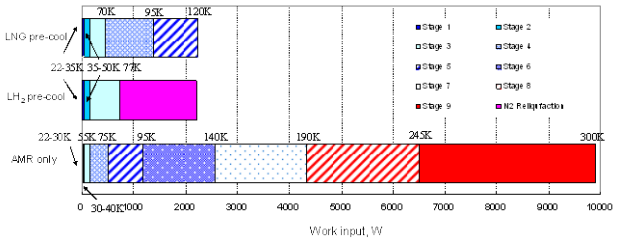

Fig. 21. Calculated total work inputs for 9 stages AMR, 3 stages AMR plus LN_2 precool and 5 stages AMR plus LNG precool.

5.2. Simulation Results

Figure 21 shows the calculated total work inputs for 9 stages AMR, 3 stages AMR plus LN_2 precool and 5 stages AMR plus LNG precool, which are 9.90 kW, 2.21 kW, and 2.23 kW, respectively. Note that these results do not include the input work for liquefaction stage by the CMR. The results clearly show that the 9 stages AMR covering from room temperature to 22 K needs considerably large

work input compared with those of the 3 stages AMR plus LN_2 precool and the 5 stages AMR plus LNG precool. On the other hand, there is a small difference on the work input between the 3 stages AMR plus LN_2 precool and the 5 stages AMR plus LNG precool. This is because the case of LN_2 precool includes the work of refrigeration to provide the LN_2, while the case of LNG suppose already to exist the cold LNG without any refrigeration. However, the 5 stages AMR plus LNG precool will be more practical system for the country like Japan because we import large amounts of LNG and we can use it as the cold heat source.

Let's estimate the efficiency for the minimum work input, i.e., the 3 stages AMR plus LN_2 precool. By our experimental results on the liquefaction stage, we assume that %Carnot of CMR is 50 %, therefore, the work input for CMR is 0.01 kW. The work input for 3 stages AMR to cool the exhaust heat from CMR is 1.30 kW from numerical simulation. Thus, we can calculate the total work input for hydrogen liquefaction as 3.52 kW.

The FOM can be obtained by dividing the minimum work, 1.65 kW, to total work input, 3.52 kW, therefore, the FOM of the hydrogen magnetic refrigeration system is 0.47. This value shows the high potential of the magnetic refrigeration system for hydrogen liquefaction, but it is noticeable that using the many stages of AMR starting from room temperatures will not provides the merit of magnetic refrigeration on the efficiency. This indicates that we need more efficient AMR system especially for room temperatures.

6. CONCLUSION

This paper reviews the status of magnetic refrigeration for hydrogen liquefaction. Technology development level stays in early stage, but the simulation results based on the experimental parameters show somewhat positive aspects. The authors also emphasize that the cost for built and operation will be able to decrease compared with the current conventional system, because the magnetic refrigeration does not require large compressors. Also the compact hydrogen magnetic refrigeration system will be interested to realize for on-site hydrogen liquefaction. Hydrogen is one of most important energy sources in the near future, so we need to prepare alternate option for hydrogen liquefaction and magnetic refrigeration is one of the candidates.

ACKNOWLEDGMENT

A part of financial supports provided by NEDO in the Search and Research of Innovative and Leading Technologies project, is greatly appreciated.

REFERENCES

[1] Required energy to compress the hydrogen gas at 70 MPa is about 15 % of HHV, 21 MJ/kg. Minimum work for hydrogen liquefaction is 12 MJ/kg, so we can estimate the FOM as 12 / 21 = 0.57.

[2] T. Utaki, T. Nakagawa, T. Yamamoto, K. Kamiya, T. Numazawa, "Research of Magnetic Refrigeration Cycle for Hydrogen Liquefaction," *Cryocooler*, vol. 14, pp. 645, 2007.

[3] T. Numazawa, K. Kamiya, S. Yoshioka, H. Nakagome, K. Matsumoto, "Development of a magnetic refrigerator for hydrogen liquefaction," AIP Conference Proceedings, vol. 985, pp. 1183-1189K, 2008.

[4] Kamiya, T. Numazawa, H. Takahashi, H. Nozawa and T. Yanagitani, "Hydrogen Liquefaction by Magnetic Refrigeration," Cryocoolers 14, Kluwer Academic/Plenum Publishers, New York, pp. 637, 2007.

[5] K. Matsumoto and T. Numazawa, "Magnetic refrigerator for hydrogen liquefaction," *Journal of Physics: Conference Series*, vol. 150, pp. 012028, 2009.

[6] K. Matsumoto, A. Matsuzaki, K. Kamiya and T. Numazawa, "Magnetocaloric Effect Specific Heat and Entropy of Iron-Substituted Gadolinium Gallium Garnets $Gd_3(Ga_{1-x}Fe_x)_5O_{12}$," *Jpn. J. Appl. Phys.*, vol. 48[11], pp. 113002-1, 2009.

[7] Y. Kim, I. Park and S. Jeong, "Experimental Investigation Of Two-Stage Active Magnetic Regenerative Refrigerator Operating Between 77 K And 20 K," *Cryogenics*, Available online 22 June 2013.

[8] A. Rowe and A. Tura, "Cryogenic testing of an active magnetic regenerative refrigerator," AIP Conf. Proc. 985, pp. 1292-1298.